https://doi.org/10.5194/acp-2021-23
Preprint. Discussion started: 1 March 2021

Atmospheric Chemistry and Physics Discussions

Evaluation of the contribution of new particle formation to cloud droplet in urban atmosphere

Sihui Jiang[1], Fang Zhang[1*], Jingye Ren[1], Lu Chen[1], Xing Yan[1], Jieyao Liu[1], Yele Sun[2], Zhanqing Li[3]

[1]College of Global Change and Earth System Science, Beijing Normal University, Beijing 100875, China

[2]State Key Laboratory of Atmospheric Boundary Layer Physics and Atmospheric Chemistry, Institute of Atmospheric Physics, Chinese Academy of Sciences, Beijing, China

[3]Earth System Science Interdisciplinary Center and Department of Atmospheric and Oceanic Science, University of Maryland, College Park, Maryland, USA

Correspondence to: F. Zhang, ***fang.zhang@bnu.edu.cn;***

Abstract

New particle formation (NPF) is a large source of cloud condensation nuclei (CCN) and cloud droplet in the troposphere. In this study, we quantified the contribution of NPF to cloud droplet number concentration (CDNC, or N_d) at typical updraft velocities (V) in clouds using a field campaign data of aerosol number size distribution and chemical composition observed on May 25-June 18, 2017 in urban Beijing. We show that the NPF drives the variations of CCN and cloud droplet and increases N_d by 30-33% at V= 0.3-3 m s^{-1} in urban atmosphere. A markedly reduction in N_d is observed due to water vapor competition with consideration of actual environmental updraft velocity, decreasing by 11.8±5.0% at V=3 m s^{-1} and 19.0±4.5% at V=0.3 m s^{-1} compared to that from a prescribed supersaturation. The effect of water vapor competition becomes smaller at larger V that can provide more sufficient water

https://doi.org/10.5194/acp-2021-23
Preprint. Discussion started: 1 March 2021

vapor. Essentially, water vapor competition led to the reduction in N_d by decreasing the environmental maximum supersaturation (S_{max}) for the activation of aerosol particles. It is shown that S_{max} was decreased by 14.5-11.7% for V=0.3-3 m s^{-1}. Particularly, the largest suppression of cloud droplet formation due to the water vapor competition is presented at extremely high aerosol particle number concentrations. As a result, although a larger increase of CCN-size particles by NPF event is derived on clean NPF day when pre-existing background aerosol particles are very low, there is no large discrepancy in the enhancement of N_d by NPF between the clean and polluted NPF day. We finally show a considerable impact of the primary sources when evaluating the NPF contribution to cloud droplet based on a case study. Our study highlights the importance of fully consideration of both the environmental meteorological conditions and multiple sources (i.e. secondary and primary) to evaluate the NPF effect on clouds and the associated climate effects in polluted regions.

1 Introduction

In the global climate system, aerosols, cloud condensation nuclei (CCN) and cloud droplets are very important components. Clouds, serving as a bridge connecting aerosols and climate, are the most uncertain factor of climate change (IPCC, 2013; Seinfeld et al., 2016; Cai et al., 2020). The microphysical link between aerosols and clouds as the most important part has received extensive attention. Cloud droplet activation is a key process from aerosol to clouds, and there has been a lot of researchers trying to simulate the microphysical processes by using parametric model (e.g. Boucher and Lohmann., 1995; Abdul-Razzak et al., 1998; Kiehl,1999; Khvorostyanov and Curry., 1999; Abdul-Razzak and Ghan., 2000; Nenes et al., 2002, 2004; Petters et al., 2007; Ren et al., 2018; Genz et al., 2020).

As a main source of aerosols, new particle formation events (NPF) have been observed and

https://doi.org/10.5194/acp-2021-23
Preprint. Discussion started: 1 March 2021

occurred frequently in different atmospheric environments in the world (Spracklen et al., 2010; Yue et al., 2011; Peng et al., 2017; Kerminen et al., 2018; Bousiotis et al., 2019; Zimmerman et al., 2020). The contribution of nucleation events to global aerosol number concentrations (or condensation nuclei, CN) cannot be ignored, as NPF contributed 81% of the aerosols in the Marine environment and 64% in the terrestrial environment (Merikanto et al., 2010). When these nucleated particles are mixed within the planetary boundary layer, they may subsequently grow to CCN-relevant sizes, or act as CCN in convective clouds (Fan et al., 2013; Li et al., 2010). In reality, from field studies, these fine particles caused by NPF can subsequently turn into an enhancement in CCN number concentration (N_{CCN}) at cloud-relevant supersaturations (Kalkavouras et al., 2017; Peng et al., 2014; Wu et al., 2015; Ma et al., 2016; Li et al., 2017; Zhang et al., 2019). But researchers have different considerations on the definition of NPF events, as well as the initiation and duration of NPF (Dal Maso et al., 2005; Leino et al.. 2016). As a result, the calculation methods about N_{CCN} enhancement during the NPF differ among the studies (Asmi et al., 2011; Kerminen et al., 2012; Peng et al., 2014).

Moreover, clouds are not characterized by a constant supersaturation. The cloud droplet number concentration (CDNC, or N_d) depends on the size distribution, chemical properties of aerosol and the cloud updraft velocity, all of which also define the maximum supersaturation (S_{max}) that can be formed in a cloud parcel (Nenes and Seinfeld, 2003). Studies have shown that the CDNC in clouds exhibits a sublinear response to aerosol particle increases (Twomey, 1977; Leaitch et al., 1986; Ghan et al., 1993; Boucher and Lohmann, 1995; Nenes et al., 2001; Ramanathan et al., 2001; Sullivan et al., 2016), as is different from CCN due to the limitation of the water vapor in the actual environment. Using the prescribed supersaturation to calculate CDNC may therefore provide a bias on evaluation the aerosol indirect effect. For example, Kalkavouras et al. (2017, 2019) reported the average 12% enhancement

https://doi.org/10.5194/acp-2021-23
Preprint. Discussion started: 1 March 2021

of CDNC during two consecutive NPF episodes in the eastern Mediterranean (Santorini and Finokalia) during summer, and this enhancement was significantly smaller than the enhancement of N_{CCN} (~87%) during the NPF day. Hence, it is critical to fully consider the background meteorological conditions (e.g. using dynamic water vapor under different updraft velocities) to simulate the S_{max} when evaluating the effect of NPF on clouds and the associated climate effects.

Relevant studies have been carried out in clean regions, but fewer in polluted urban areas. While field studies have shown that NPF events can occur frequently in polluted urban sites although the high concentration of background particles are not conducive to the generation of new particles (Wu et al., 2011; Peng et al., 2014; :Zimmerman et al., 2020), and its characteristics like nucleation, growth rate, final size and environmental effect may be larger than that of relatively clean atmosphere. Wiedensohler et al. (2012) also found, under the high concentration levels of gaseous pollutants and strong oxidation in polluted area, the high concentration of nanoparticles generated by NPF events can rapidly grow to tens or even hundreds of nanometers in a few hours. Zhang et al. (2019) observed the subsequent growth of newly formed particles can last 2-3 days in urban Beijing, producing more CCN-sized particles. Previous studies in polluted regions demonstrated the complex and non-linear relationship between aerosol particles and CCN due to multiple emission sources (Zhang et al., 2014, 2016, 2017, 2019; Ren et al., 2018; Fan et al., 2020), highlighting the importance of understanding of the connections between aerosols and CCN or cloud droplet close to the source regions. Particularly, owing to the extremely high CN number concentrations (with order of magnitude as high as 10^4 or even 10^5 cm^{-3}) during NPF events in urban area, the effect of competition for water vapor and reduction in cloud supersaturation is expected to be more exacerbated.

The current study quantifies the contribution of NPF to CCN and CDNC in the polluted urban

https://doi.org/10.5194/acp-2021-23
Preprint. Discussion started: 1 March 2021

atmosphere of Beijing using field measurements of aerosol number size distributions and chemical composition. We aim to investigate the NPF impacts on N_d and S_{max} formed in clouds by applying five updraft velocities. Effect of the background pre-existing particles on the enhancement of CCN and CDNC is also discussed by contrasting the results on typical "clean" NPF day and "polluted" NPF day. Given the influence of strong local primary sources like traffic emissions in urban area, a case study has been done finally to evaluate the interference from evening rush hour.

2 Methodology

2.1 Experimental site

A field campaign was conducted from May 25, 2017 to June 18, 2017 at the Institute of Atmospheric Physics (IAP), Chinese Academy of Sciences (39.98° N, 116.39° E) for measurements of aerosol physical and chemical properties. The IAP located between the north Third Ring Road and Fourth Ring Road in northern Beijing, which is a typical urban background site, mainly affected by traffic and catering emissions. Beijing is hot in summer with high ambient relative humidity, which is conductive to generate atmospheric convection and reduce the high background aerosol condensation sink. And the radiation in summer is relatively strong, which promotes the generation of nucleated particles. Besides, local sources from traffic and cooking emissions, which may contribute many CCN-size particles, can be important at the site (Sun et al., 2015).

2.2 Measurements of aerosol size distribution and chemical composition

The number size distribution of particles in the size range from 10 to 550 nm (scanned range) were measured with time resolution of 5 minutes by a scanning mobility particle sizer (SMPS; Wang and Flagan, 1990; Collins et al., 2002) , which consists of a differential mobility analyzer (DMA, model 3081L, TSI Inc.) to classify particles with different particle sizes, and a condensation particle

https://doi.org/10.5194/acp-2021-23
Preprint. Discussion started: 1 March 2021

counter (CPC, model 3772, TSI Inc.) to detect the size-classified particles. The sampled particles were dried to a relative humidity < 30% before entering the DMA. According to the particle number size distribution (PNSD), we can identify the NPF event by a typical "banana" shape (Kalkavouras et al., 2019) with a sudden increase of nucleated particle number (10-30 nm) and further grow into larger particles over a short time period (usually less than 4 h). While non-NPF events may also have sudden increases of nucleated particles at a short time scale, but they do not show further growth.

The non-refractory chemical composition of PM_1 is measured by an Aerosol Chemical Speciation Monitor (ACSM), which consists of an aerodynamic lens to efficiently sample and focus submicron particles into the ACSM (Ng et al. 2011). And the measurements were deployed at ground level and at the 260 m level of the tower (Du et al., 2017), Before sampling into the ACSM, aerosol particles are dried by silica gel desiccant. The ACSM was operated at a time resolution of 15 min. And the non-refractory chemical components that can be measured mainly include organics, sulfate salts (SO_4^{2-}), nitrate salts (NO_3^-), ammonium (NH_4^+), and chloride (Cl^-) (Ng et al. 2011). The refractory components mainly include Black carbon (BC), the BC mass concentration was measured using a seven-wavelength aethalometer (AE33, Magee Scientific Corp) .

2.2 Calculation of CCN number concentrations

According to the hygroscopic growth process of particles described by Köhler theory (Köhler et al., 1936), with the growth of particles, their surface water vapor phase equilibrium (supersaturation ratio) will gradually increase. When they grow to a certain size, the required equilibrium supersaturation ratio will not increase, but will decrease. This means the system reaches a critical point, at which the corresponding particle size and supersaturation ratio are called critical diameter (d_c) and critical supersaturation (S_c). Beyond this critical point, particles can condense and grow spontaneously

https://doi.org/10.5194/acp-2021-23
Preprint. Discussion started: 1 March 2021

without increasing the S_c. Therefore, if a particle grows to a critical particle size at or above the critical S_c, the particle is activated to form a cloud droplet.

In calculation, the corresponding minimum particle size (d_m) can be obtained according to a prescribed environmental supersaturation, and all particles with particle size larger than the d_m can be activated. So CCN number concentrations can be calculated by integrating the PNSD from d_m to the largest particle size measured:

$$CCN(d_c) = \int_{dc}^{\infty} n(d_p)ddp \approx \sum_{dm}^{550} \Delta N_i, \quad (1)$$

$$d_c = (\frac{4A^3}{27\kappa s_c^2})^{1/3}, A = \frac{4M_W\sigma_W}{RT\rho_W}, \quad (2)$$

In κ-Köhler formula (5), κ is a hygroscopic parameter which depends on the chemical composition of the particle. In this study, we derived the hygroscopic parameter, κ, by a simple mixing rule on the basis of chemical volume fractions under the assumption of internal mixture (Petters and Kreidenweis, 2007; Gunthe et al., 2009). We used ACSM data to calculate the volume fraction of organic and inorganic, according to the next calculation rule:

$$\kappa_{chem} = \sum_i \varepsilon_i \kappa_i, \quad (3)$$

where κ_i and ε_i are the hygroscopic parameter and volume fraction for each individual (dry) component in the mixture, respectively.

2.3 Calculation of cloud droplet number concentrations

The cloud droplet number depends on the S_{max} that can be formed in adiabatic ascending clouds, since this "cloud-relevant" supersaturation is not fixed, it is limited by the competition of water vapor. Nenes and Seinfeld et al (2003, 2004) established a global cloud parametric model based on the "population splitting" concept, which was later improved by Fountoukis and Nenes (2005). The S_{max} was calculated from an equation that expresses the water vapor balance in adiabatic ascending cloud

https://doi.org/10.5194/acp-2021-23
Preprint. Discussion started: 1 March 2021

(Nenes and Seinfeld., 2003):

$$\frac{ds}{dt} = \alpha V - \gamma \frac{dw}{dt}, \tag{4}$$

where α and γ are two coefficients can be calculated by meteorological constants, the first term on the right side of equation (7) expresses the increase of supersaturation due to the adiabatic cooling of the parcel, while the second term expresses the decrease of supersaturation due to the depletion of water vapor by the activated droplets. And the left side express the growth rate of supersaturation, when it is equal to 0, the supersaturation reaches the maximum value.

Nenes et al.(2001) used a sectional representation of the CCN spectrum (i.e. aerosol supersaturation distribution $n^s(s')$) and total number of particles with critical supersaturation smaller than s, $F^S(S)$, which is given by

$$F^S(s) = \int_0^s n^s(s')ds' = \sum_{j=1}^{i-1} N_j + N_i\left(\frac{s - s_{c,i-1}}{s_{c,i} - s_{c,i-1}}\right), \tag{5}$$

If the maximum supersaturation (S_{max}) is known, the activated cloud droplet number (N_d) can be calculated from equation (8), as

$$N_d = F^s(s_{\max}), \tag{6}$$

In this study, we used the PNSD, chemical components, and empirical values of cloud updraft velocity to determine the S_{max} and N_d during NPF days in urban Beijing. Owing to that calculation of cloud updraft velocity is almost impossible, the typical cloud updraft velocity (ranging from 0.3 to 3 m s^{-1}) that can represent the conditions of different clouds types (stratocumulus/cumulus and convective clouds) in summer of north China is applied here according to field observation or empirical data (Morales and Nenes. 2010; Zheng et al., 2015).

https://doi.org/10.5194/acp-2021-23
Preprint. Discussion started: 1 March 2021

3 Results and discussion

3.1 Time series of observed NPF events and calculated N_{CCN} and N_d

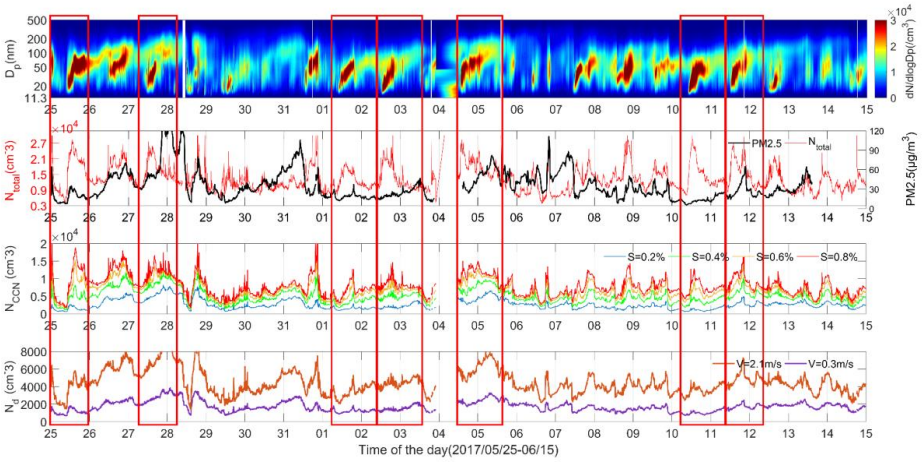

Figure 1. Time series of the (from top to bottom) particle number size distribution (PNSD) (typical NPF events are marked in red box), particle number concentration (N_{total}), particle mass concentration ($PM_{2.5}$), CCN number concentration (N_{CCN}), and cloud droplet number concentration (N_d). Data are from 25 May to 15 June 2017. The different colors for N_{CCN} represent the calculated value under different supersaturations (S) (the S of 0.2%, 0.4%, 0.6%, 0.8% corresponds to the colors in blue, green, yellow, red respectively). And different colors of N_d represent the results at different updraft vertical velocity (V) (the V of 0.3 m s^{-1}, 2.1 m s^{-1} corresponds to the colors in orange and purple respectively).

As a typical NPF event includes the sudden increase of nucleation particles (10-25 nm), the subsequent growth of the newly formed particle, the duration of the event (more than two hours) and the terminal of the NPF event (Leino et al., 2016), NPF events in total, accounting for about half of the observation time, occurred during the studied periods. Here, we just select 7 NPF events to study as

https://doi.org/10.5194/acp-2021-23
Preprint. Discussion started: 1 March 2021

marked in red box in Fig. 1.

Fig. 1 also presents the time series of N_{CCN} and N_d. The N_{CCN} has a strong response to aerosol increase during the NPF events as expected, and this response always occurs a few hours after the start of NPF, as the growth of nucleation mode particles to sufficient size (Aitken mode or accumulation mode) (Fig. 2). The variation of N_{CCN} seems to be more consistent with that of N_{CN} than N_d. Since the N_{CCN} was calculated based on an assumption that the water vapor in the environment is always sufficient, the increase of N_{CN} which indicates the occurrence of NPF events can bring more CCN as shown in Fig. 1. However, due to the pre-existing aerosol in the background, which may contribute a large amount of CCN, it is necessary to consider a time node (t_{dec}) when NPF begin to impact N_{CCN} and the duration of this effect (Kalkavouras et al., 2019) when we evaluating the CCN enhancement caused by NPF.

Therefore we used the methods of Kalkavouras et al(2019) to calculate the "decoupling time", t_{dec}, in the selected seven typical NPF days, and we found t_{dec} occur 2-3 hours later after t_{start} in most of NPF days. So we took the period from 12:00 to 16:00 to estimate the change of CCN during NPF events (the end time is taken as 16:00 to avoid the interference of evening traffic emissions). According to the time nodes determined above, we defined the enhancement percentage of CCN number concentration as the ratio of the average increment of CCN during NPF period to the average concentration of pre-NPF events. The enhancements in CCN number from NPF were calculated for 0.2%, 0.4%, 0.6%, 0.8% supersaturation, with the average values of 33.9%, 42.3%, 53.4%, and 76.3%, respectively (Table S1 and Figure 2b). As a result, we show that the NPF drives the variance of N_{CCN}, and 24.4%, 26.1%, 32.4%, 40.3% of environment total CCN are directly originated from NPF at 0.20%, 0.4%, 0.6%, 0.8% supersaturation respectively, suggesting large source of CCN from NPF events. And

https://doi.org/10.5194/acp-2021-23
Preprint. Discussion started: 1 March 2021

about 60-75% CCN are from the background pre-existing particles in urban Beijing, which is much larger than that derived in remote Finokalia, Crete, Greece by Kalkavouras et al (2019).

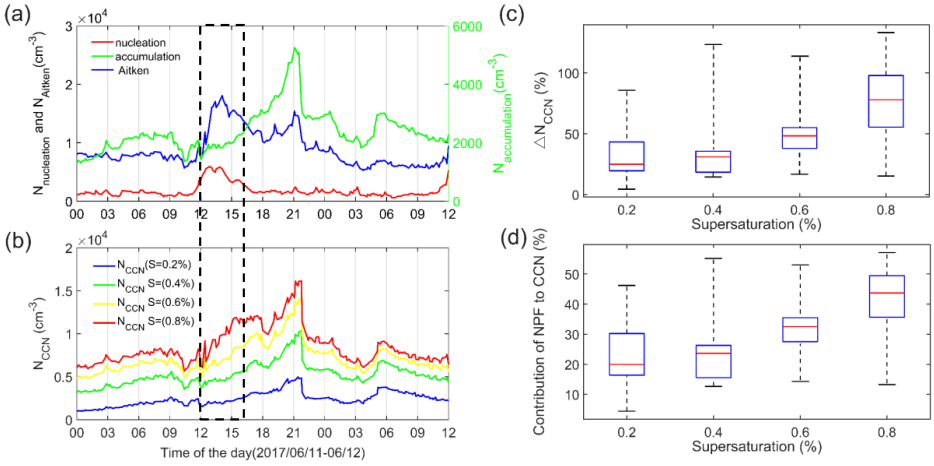

Figure 2. (a) Diurnal evolution of nucleation (10-25 nm, red line), Aitken (25-100 nm, blue line), and accumulation mode(>100 nm, green line) particle number concentration on 11 June 2017, respectively; (b) Diurnal evolution of CCN number concentration under different supersaturation(0.2%-0.8%); (c) Box diagram for the average enhancement of CCN caused by NPF under different supersaturation (0.2%-0.8%) on all NPF days; (d) Box diagram for the average contribution of NPF to CCN under different supersaturation (0.2%-0.8%) on all NPF days.

3.2 Impact of NPF on cloud droplet number in Beijing

The estimated results of S_{max} and N_d for two selected vertical updraft velocity of V=0.3 m s^{-1} and V=2.1 m s^{-1} on 11 June 2017 are shown in Fig. 3a and Fig. 3b. Generally, the S_{max} was calculated to be under 0.4% and 0.2% for V=2.1 m s^{-1} and V=0.3 m s^{-1} respectively, and the corresponding critical particle sizes (d_c) are 70 nm and 110 nm. It means that most activated drops are from accumulation-mode particles and larger particles in Aitken-mode. The large contribution of the Aitken-mode particles lead to large amount of cloud droplets in urban Beijing, especially for high updraft velocity. Basically,

https://doi.org/10.5194/acp-2021-23
Preprint. Discussion started: 1 March 2021

the number concentration of cloud droplets is above 1000 cm^{-3}, which is of a much larger magnitude compared with that in the clean areas (Morales et al., 2014; Sullivan et al.,2016; Kalkavouras et al., 2019).

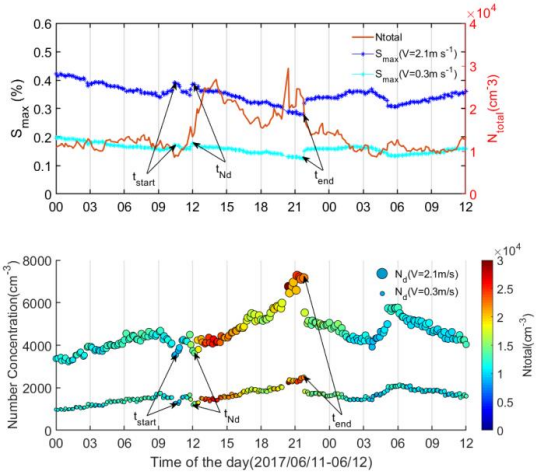

Figure 3. (a) Diurnal evolution of the maximum supersaturation (S_{max}) in the cloud for updraft velocities of 2.1 m s^{-1} and 0.3 m s^{-1}, and the total aerosol particle number concentrations in cm^{-3} (N_{total}, right axis); **(b)** Diurnal evolution of calculated cloud droplet number concentrations (N_d) (left axis) for updraft velocities of 2.1 m s^{-1} and 0.3 m s^{-1}.

In the cloud, the change in the quantity of particles can be directly reflected by the change in S_{max}, as shown in Fig. 3. The rise of environmental supersaturation means that the water vapor in the air mass is sufficient, that suggests the water vapor produced by the adiabatic rise of clouds is more than the water vapor consumed by the condensation of particles. When the production equals to the consumption of water vapor, the water vapor in air mass reaches a balance, and the environmental supersaturation stops increasing. With the further growth of the CCN to form droplets, more water vapor will be consumed, this equilibrium will be broken and the environmental supersaturation will begin to decrease. This moment indicates the cloud droplets in air mass begin to "feel" the particles

https://doi.org/10.5194/acp-2021-23
Preprint. Discussion started: 1 March 2021

generated from NPF, for example, the N_d rapidly increased from ~4000 to nearly 8000 cm^{-3} over 9 hour period starting at 12:00 am (Fig. 3b). This moment at 12:00 a.m will be defined as t_{Nd}, and the time lag between t_{Start} and t_{Nd} was about 2-3 hour, which is shortened by two thirds compared to that reported by Kalkavouras et al., (2019). This case in 11 June was not an individual case, and similar patterns are also shown on other NPF days during the campaign (Fig. S4-S9).

When evaluating the impact of NPF on cloud drops, we define this impact continues until N_d begin to decrease meanwhile the S_{max} begins to increase, and we set this time node as t_{end} (the t_{end} here should be distinguished from the time node when NPF events end). Then the enhancements of cloud droplets by NPF are defined as the difference of N_d (ΔN_d) before t_{Nd} (during t_{start} and t_{Nd}) and after t_{Nd} (during t_{Nd} and t_{end}). The average enhancements under different updraft velocities are exhibited in Fig. 4a and Fig. 4b. The results show that the mean enhancements in N_d by NPF are 398, 734, 951, 1107, 1328 cm^{-3} at updraft velocities of 0.3, 0.9, 1.5, 2.1, and 3 m s^{-1} respectively, corresponding to elevated percentages of 30%, 33%, 33%, 33%, 32%. It suggests that the higher cloud updraft velocity not only generates more cloud droplets, but also induces larger enhancements in N_d. While the percentages of the enhancement remain the same from low to high updraft velocity since this value depends both on the increased quantity of cloud droplets and the concentration of pre-exist cloud droplets.

Furthermore, we estimate the changes of N_{CN} and κ to the variance of N_d under different updraft velocities (V) using Eqs. S1, S2 and S3. The results demonstrate changes in N_{CN} contributed 68% in average to the variance of N_d and this contribution increased with the increase of V, and the remaining 32% is attributed to the changes in κ (Table S3). Our calculation indicates the importance of NPF events to variations of N_d by elevating the total N_{CN} in polluted urban area.

https://doi.org/10.5194/acp-2021-23
Preprint. Discussion started: 1 March 2021

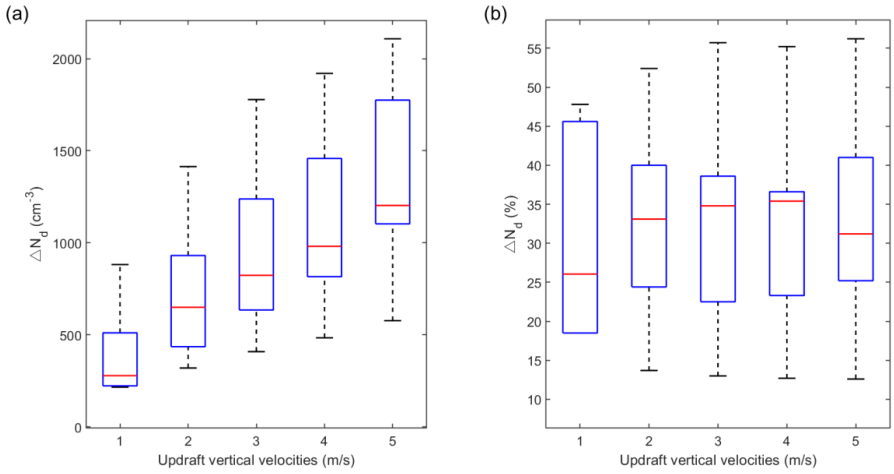

Figure 4. (a) Box diagram for the average enhancement of cloud droplets number concentration (N_d) by NPF events under different updraft vertical velocities; and (b) Box diagram for the corresponding enhanced percentages of N_d by NPF events.

3.3 The effect of water vapor competition on evaluating N_d

Fig. 5 shows the scatter plots of correlations between N_{CN} and N_{CCN} at different supersaturations and the correlations between N_{CN} and N_d under different updraft vertical velocities. The N_{CCN} and N_{CN} were obviously linear correlated, but the correlation between N_d and N_{CN} was non-linear. When showing as the average values with error bars, we find most N_d increase as N_{CN} increase when N_{CN} is below 15000, then N_d began to decrease as N_{CN} continue to increase. This has been presented in previous studies (Nenes et al., 2001; Ramanathan et al., 2001; Sullivan et al., 2016), and was thought caused by the water vapor competition. Although the larger updraft velocities generate more water vapor and can form more N_d, the water vapor competition still occurred when background aerosol particles increased to a certain number. This fully suggests the difference between the fixed supersaturation S used in the calculation of N_{CCN} and the actual supersaturation S_{max} in the air mass used in the calculation of cloud droplets. Because in the actual environment, it is often unable to

https://doi.org/10.5194/acp-2021-23
Preprint. Discussion started: 1 March 2021

provide enough water vapor. For example, the S_{max} is lower than 0.5% at the maximum cloud updraft velocity of 3 m s^{-1} according to the calculation in this study. Therefore, although NPF events may strongly increase CCN numbers, the formed cloud droplet numbers are eventually limited by water vapor availability which depends on the supersaturation (S_{max}) that can develop in the cloud. The latter is related to the cloud formation dynamics and the aerosol levels associated with the background in the region.

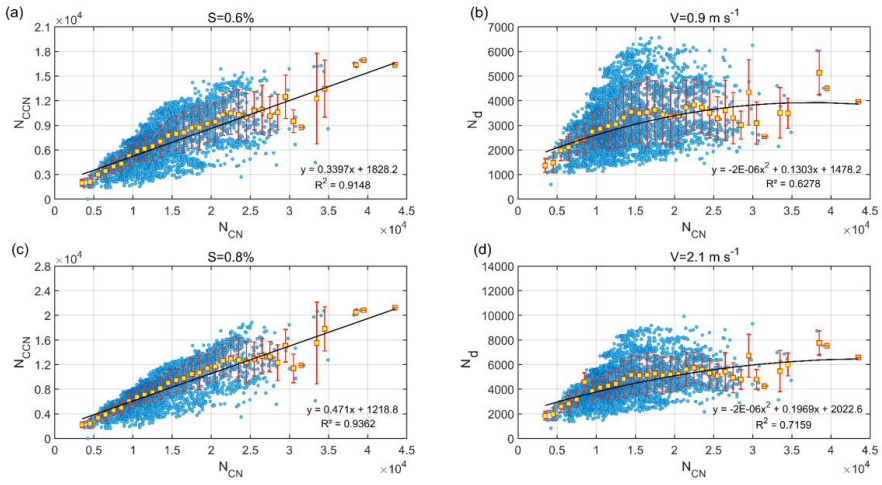

Figure 5. (a), (c) Correlation between aerosol number concentration (N_{CN}) and mean N_{CCN} at supersaturation of 0.6% and 0.8% respectively. **(b), (d)** Correlation between aerosol number concentration (N_{CN}) and mean cloud droplet number concentration (N_d) at updraft vertical velocity of 0.9 m s^{-1} and 2.1 m s^{-1} respectively.

To evaluate the effect of water vapor competition on N_d, by taking the case on 11 June as an example, we calculate and show the diurnal variation of N_d with and without the water vapor depletion in Fig. 6a. For the test, if assuming no water vapor depletion, the S_{max} would not decrease after t_{Nd} (12:00), so the ideal number of cloud drops was equal to the estimated N_{CCN} for the supersaturation of

https://doi.org/10.5194/acp-2021-23
Preprint. Discussion started: 1 March 2021

S_{max} at the time of t_{Nd}. The effect of water vapor competition under different cloud updraft velocities is assessed by comparing actual derived N_d with the ideal value from a fixed supersaturation (S_{max}) as shown in Fig. 6. The results from other NPF events were also summarized in Table S4 and Table S5. Obviously, the N_d is largely reduced due to the water vapor competition at both the low and high updraft velocity, suggesting significant suppression of cloud droplet formation, with average suppression percentages of 19.0±4.5%, 15.7±4.7%, 14.8±5.6%, 12.3±4.9%, 11.8±5.0% for N_d at updraft velocity of 0.3, 0.9, 1.5, 2.1 and 3 m s^{-1} on all NPF days. It was consistent with the results of Kalkavouras et al., 2017, they found this competition effects suppress N_d by 20% for V = 0.3 m s^{-1} and 12.3 % for V = 0.6 m s^{-1}. The declined percentages with increase of the updraft velocity suggests that the effect becomes smaller at larger V that can provide more sufficient water vapor. In addition, after the t_{Nd}, S_{max} was negatively correlated with N_d for both updraft velocities due to the increasing competition for water vapor from the growing number of droplets (Fig. 3a). Essentially, water vapor competition led to the reduction in N_d by decreasing the required S_{max} for the CN activation. It is shown that S_{max} was decreased by 14.5±3.5%, 13.3±4.0%, 13.4±4.2%, 12.0±4.1%, 11.7±3.9% for V=0.3, 0.9, 1.5, 2.1 and 3 m s^{-1} respectively.

3.4 The variations of CCN and cloud droplet on typical ”clean” and ”polluted” NPF day: a case study

Generally, the lower $PM_{2.5}$ means low background condensation sink (CS) which is conductive for nucleation particles condense and coagulate (Wu et al., 2011; Yue et al., 2011; Wiedensohler et al., 2012). Different from the remote clean area, some of the NPF events in urban Beijing during the campaign occurred with background pollutions (with daily mass concentrations of $PM_{2.5}$ of ~40 μg m^{-3}) or are impacted by local primary emissions. This kind of NPF event has different characteristics

https://doi.org/10.5194/acp-2021-23
Preprint. Discussion started: 1 March 2021

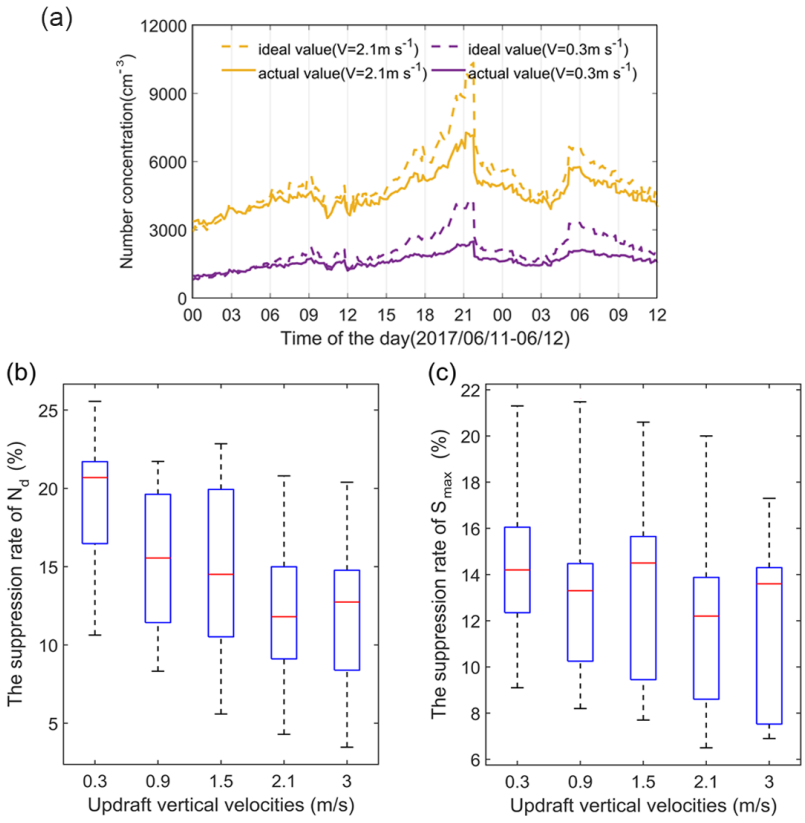

Figure 6. (a) The diurnal variation of N_d with or without considering water vapor competition at updraft speeds of 2.1 m s^{-1} and 0.3 m s^{-1} on 11 June 2017; **(b)** Box diagram for the suppression rate of N_d under different updraft vertical velocities from all selected NPF cases; **(c)** Box diagram for the suppression rate of S_{max} under different updraft vertical velocities from all selected NPF cases.

from that in clean conditions, as the sudden increase of nucleation particles less than 25 nm is often accompanied by an increase of large particles at the beginning of NPF. Here, they are named as "Polluted" and "Clean" NPF event respectively. Two days, on 27 May and 11 June, representing the typical "polluted" and "clean" NPF events respectively, are selected for contrasting the effect of the

https://doi.org/10.5194/acp-2021-23
Preprint. Discussion started: 1 March 2021

two kinds of NPF on CCN and CDNC. As shown in Fig. 7, there is a higher pre-existing background of accumulated mode particles across the day on "polluted" NPF day of 27 May than that on "clean" NPF day of 11 June. On "clean" NPF day, much more nucleation and Aitken mode particles, with N_{CN} enhancement of 7-fold higher than that on "polluted" day (Fig. 8a), were generated and NPF events developed stronger in the initial stage. The beginning of NPF events (t_{Start}) on polluted case (11:00 a.m.) was about 2 hours later than that on clean case (~9:00 a.m).

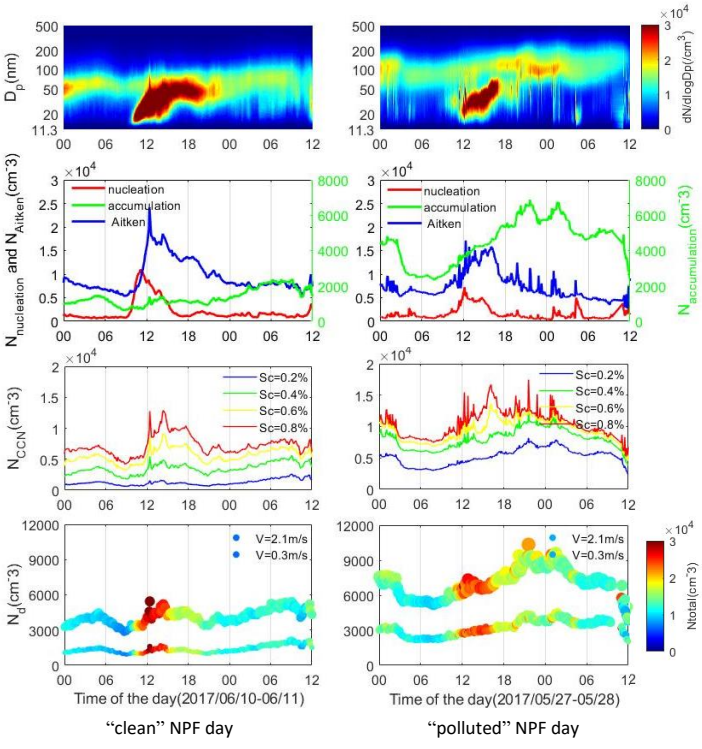

Figure 7. Comparison of two different typical NPF events, "clean" NPF day with cleaner background which $PM_{2.5}$=14 (μg/m^3) and "polluted" NPF day with $PM_{2.5}$=73 (μg/m^3). Two typical NPF days (10 June and 27 May 2017) are selected to compare the diurnal evolution trend of particles; CCN number concentration and the diurnal variation of CCN; cloud droplet number concentration and its evolution pattern under two different NPF types.

https://doi.org/10.5194/acp-2021-23
Preprint. Discussion started: 1 March 2021

For the both cases, the N_{CCN} are increased with the evolution of the NPF events (Fig. 7). But the magnitude of the enhancements at the two cases are quite different. The average CCN number concentration during NPF events under polluted day was twice than that of clean day due to that there were a large number of pre-exist CCN-size aerosol particles on polluted NPF days. While, a larger enhancement of N_{CCN} is derived on clean NPF day, showing 80-120% and 40-57% contribution of NPF to N_{CCN} on clean and polluted days respectively. This result is reasonable and consistent with the conclusion of Kalkavouras et al., 2019. However, the enhancement of N_d by NPF on polluted day was almost the same as that on clean day, with an overall enhancement of 30-40% under updraft velocity of 0.3 and 2.1 m s^{-1}. This suggests that it is critical to fully consider the background meteorological conditions (e.g. using dynamic water vapor under different updraft velocities) to simulate the cloud droplet when evaluating the effect of NPF on clouds and the associated climate effects.

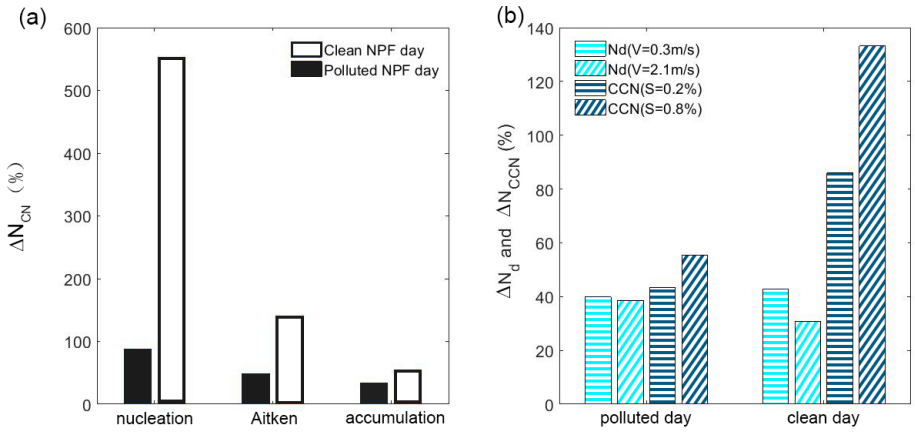

Figure 8. Comparison of two different typical NPF events, **(a)** Change of N_{CN} which is influenced by NPF, **(b)** Chang of N_d and N_{CCN}, which are estimated before and after NPF, dividing the increment by the previous amount and get the this proportion.

https://doi.org/10.5194/acp-2021-23
Preprint. Discussion started: 1 March 2021

3.5 The impact of primary emissions during evening rush hour on the calculation of NPF contribution to N_d: *a case study*

During the campaign, very high number concentrations of Aitken particles were frequently observed during evening rush hour (as shown in Fig. 9a and 9b) when primary emissions related to automobile exhaust or cooking activities near the site dominate the PNSD. This is also shown in the diurnal variations of particles chemical composition, with a large increase of primary organic aerosols (POA) and BC both in the mass concentration and fraction (Fig. 9c and 9d). The PNSD showed a major peak in the Aitken mode at ~50 nm during the rush hour time and minor peaks in Aitken (~30 nm) and accumulation (~100-120 nm) mode, which have been demonstrated related to vehicle emissions (Brines, M et al., 2015). Those primarily emitted particles can serve as CCN and thereby impact the evaluation of NPF contribution to cloud droplet. Therefore, taking the day of June 11 as an example, such effect from primary emissions during evening rush hour is investigated. On the day, after one hour of the eruption of newly formed particles at ~12:00 a.m, the N_d began to rise rapidly, and this moment was t_{Nd}, the increase of N_d continued from 12:00 until to 21:30 at night (as shown in Fig. 3a and 3b). At 18:00, the primary emissions also begin to impact the N_d. A sudden decrease and dilution in the PNSD is due to a precipitation event at 21:30. From 18:00-21:30, the cloud droplets were from both NPF source and the primary emissions.

https://doi.org/10.5194/acp-2021-23
Preprint. Discussion started: 1 March 2021

Atmospheric Chemistry and Physics Discussions

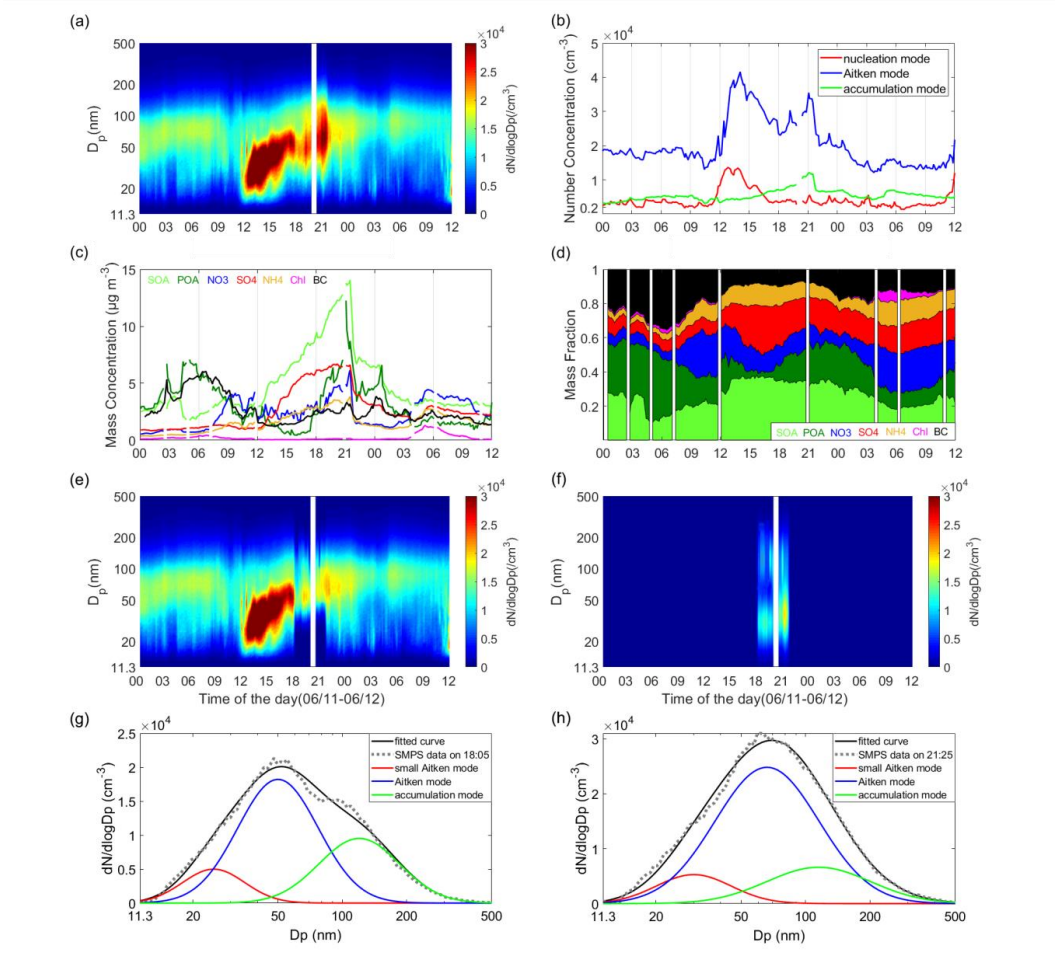

Figure 9. (a) Diurnal evolution of the aerosol size distribution; **(b)** Diurnal evolution of nucleation (red line), Aitken (blue line), and accumulation mode particle number concentration (green line), respectively; **(c)** Diurnal evolution of the aerosol chemical composition include (BC, NH_4, NO_3, POA, SOA, SO_4, Chl); **(d)** Mass fraction of aerosol composition; **(e)** Diurnal evolution of particle number size distributions without considering primary emission; **(f)** Diurnal evolution of particle number size distributions only considering primary emission during 18:05-21:25; **(g)** and **(h)** fitted results of the particle number size distributions at 18:05 and 21:25 respectively

https://doi.org/10.5194/acp-2021-23
Preprint. Discussion started: 1 March 2021

Table 1. Impact of primary emissions on evaluating the contribution of NPF to N_d increment

V, m s^{-1}	D_c, nm	$\triangle N_{d\_NPF}$, cm^{-3}, %		$\triangle N_{d\_PE}$ [a], cm^{-3}, %		$\triangle N_{d\_total}$, cm^{-3}
0.3	140	241	86.4%	38	13.6%	279
0.9	107	555	82.6%	117	17.4%	672
1.5	93	613	75.8%	196	24.2%	809
2.1	84	675	69.6%	295	30.4%	970
3	75	862	70.9%	354	29.1%	1216

[a]PE, primary emission

It is expected that the newly formed particles continued to grow until 21:30, we estimate the size mode of the newly formed particles after 18:00. In this case, a value of 3.2±0.5 nm h^{-1}, which is the growth rate of the newly formed particles during 12:00-18:00, is applied for the estimation. The calculation results show that the new particles can grow to ~50 nm at 18:05 and ~60 nm at 21:25. So we can get the PNSD of NPF and primary emissions respectively (Fig. 9e and 9f) by fitting the three modes assuming a normal distribution. Fig. 9g and Fig. 9h show the fitted results of the three modes of the PNSD at 18:05 and 21:25 respectively . Then the increment of N_d from NPF are obtained from the PNSD of NPF. In addition, the chemical composition of newly formed particles during evening rush hour is assumed same to that at 18:00 to calculate the κ and the critical diameter. Finally, the increment of N_d from primary emissions are obtained by subtracting the increment of N_d by NPF from the total increment of N_d. When calculating the enhancement of N_d by NPF, the N_d before t_{Nd} (during 09:00-12:00), taking as a background, was directly subtracted from the total N_d by NPF after t_{Nd} (during

https://doi.org/10.5194/acp-2021-23
Preprint. Discussion started: 1 March 2021

12:00-21:30). The calculated results are summarized in Table 1. The average contribution of primary emission to N_d is 13.6%, 17.4%, 24.2%, 30.4% and 29.1% cm^{-3} for updraft velocities of 0.3, 0.9, 1.5, 2.1 and 3 m s^{-1} respectively. The proportion of contribution from NPF and primary emission to N_d increment change with the variation of updraft vertical velocity (V). The higher proportion of contribution from primary emission is obtained at higher V, which may be determined by the different characteristics between atmospheric particles emitted from the evening traffic sources and generated from NPF events. Our result shows considerable impact of those primary sources when evaluating the NPF contribution to cloud droplet, highlighting the importance of considering the influence from multiple (i.e. secondary and primary) sources on clouds in the polluted atmosphere.

4 Conclusions

In this study, we quantified the contribution of NPF to cloud droplet number concentration (CDNC, or N_d) at typical updraft velocities in clouds using field measurements of aerosol number size distributions and chemical composition in urban Beijing. We show that the NPF drives the variations of CCN and cloud droplet. About 25%-40% CCN are from NPF events in polluted atmosphere. And the N_d is increased about 30%-33% by NPF at V= 0.3-3 m s^{-1} accordingly. The markedly reduction in N_d is observed due to water vapor competition with consideration of actual environmental updraft velocity, with decrease rates of 11.8%±5.0% at V=3 m s^{-1}and 19.0%±4.5% at V=0.3 m s^{-1} by comparing with that from a prescribed supersaturation. The effect of water vapor competition becomes smaller at larger V that can provide more sufficient water vapor. Essentially, water vapor competition led to the reduction in N_d by decreasing the environmental S_{max} for the activation of aerosol particles. It is shown that S_{max} was decreased by 14.5 ± 3.5% to 11.7 ± 3.9% for V=0.3-3 m s^{-1}. Our results suggest significant suppression of cloud droplet formation due to the water vapor competition particularly at

https://doi.org/10.5194/acp-2021-23
Preprint. Discussion started: 1 March 2021

extremely high aerosol particle number concentrations. As a result, although a larger increase of CCN-size particles by NPF event is derived on clean NPF day when pre-existing background aerosol particles are very low, no large discrepancy in the enhancement of N_d by NPF between the clean and polluted NPF day. Finally, we show a considerable impact of the primary sources when evaluating the NPF contribution to cloud droplet from a case study. Our study highlights the importance of fully consideration of both the environmental meteorological conditions and multiple sources (i.e. secondary and primary) to evaluate the effect of NPF on clouds and the associated climate effects. For example, Merikanto et al. 2010 used model to simulate the variance of CDNC from the year of 1850 to 2000, and showed that NPF made a nearly equal contribution (16-13.5%) to global CDNC in all those years, leading to ~50% enhancement in the year from1850 to 2000 change in cloud albedo. There are still large uncertainties about how to accurate quantitatively assess the response of these climate effects to NPF. This study is carried out in polluted area, which is a supplement to the related cloud microphysical progress research and provides a new perspective for the follow-up research.

Acknowledgments

This work was supported by the National Basic Research Program of China (2017YFC1501702), the National Natural Science Foundation of China (Grants 41675141, 41975174). All data used in the study are available on https://data.mendeley.com/datasets/hkkzbn4zv3/1 or from the corresponding author upon request (fang.zhang@bnu.edu.cn).

The authors declare no competing financial interest.

Author contribution

FZ and SJ conceived the conceptual development of the paper. LC, YS and JR contributed

measurements. SJ directed and performed the experiments with LC, JL, JR, XY, ZL and FZ, SJ conducted the data analysis and wrote the draft of the paper. All authors commented on the paper.

References

Albrecht, B. A.: Aerosols, cloud microphysics, and fractional cloudiness, Science, 245, 1227–1230, 1989.

Abdul-Razzak, H., Ghan, S., and Rivera-Carpio, C.: A parametreization of aerosol activation: 1. Single aerosol types, J. Geophys. Res., 103, 6123–6131, 1998.

Abdul-Razzak, H. and Ghan, S.: A parametreization of aerosol activation: 2. Multiple aerosol types, J. Geophys. Res., 105, 6837–6844, 2000.

Asmi, E., Kivekäs, N., Kerminen, V.-M., Komppula, M., Hyvärinen, A. P., Hatakka, J., Viisanen, Y., and Lihavainen, H.: Secondary new particle formation in Northern Finland Pallas site between the years 2000 and 2010, Atmos. Chem. Phys., 11, 12959–12972, https://doi.org/10.5194/acp-11-12959-2011, 2011.

Boucher, O. and Lohmann, U.: The sulfate-CCN-cloud albedo effect, Tellus, 47B, 281–300, 1995.

Bousiotis, D., Dall'Osto, M., Beddows, D. C. S., Pope, F. D., and Harrison, R. M.: Analysis of new particle formation (NPF) events at nearby rural, urban background and urban roadside sites, Atmos. Chem. Phys., 19, 5679–5694, https://doi.org/10.5194/acp-19-5679-2019, 2019.

Brines, M., Dall'Osto, M., Beddows, D. C. S., Harrison, R. M., Gómez-Moreno, F., Núñez, L., Artíñano, B., Costabile, F., Gobbi, G. P., Salimi, F., Morawska, L., Sioutas, C., and Querol, X.: Traffic and nucleation events as main sources of ultrafine particles in high-insolation developed world cities, Atmos. Chem. Phys., 15, 5929–5945, https://doi.org/10.5194/acp-15-5929-2015, 2015.

Cai, M., Liang, B., Sun, Q., Zhou, S., Chen, X., Yuan, B., Shao, M., Tan, H., and Zhao, J.: Effects of continental emissions on cloud condensation nuclei (CCN) activity in the northern South China Sea during summertime 2018, Atmos. Chem. Phys., 20, 9153–9167, https://doi.org/10.5194/acp-20-9153-2020, 2020.

Collins, D. R., Flagan, R. C., and Seinfeld, J. H.: Improved inversion of scanning DMA data, Aerosol Sci. Tech., 36, 1–9, 2002.

Dal Maso, M., Kulmala, M., Riipinen, I., Wagner, R., Hussein, T., Aalto, P. P., and Lehtinen, K. E. J.: Formation and growth of fresh atmospheric aerosols: eight years of aerosol size distribution data from SMEAR II, Hyytiälä, Finland, Boreal Environ. Res., 10, 323–336, 2005.

Fan, J., Leung, R., Rosenfeld, D., Chen, Q., Li, Z., Zhang, J., and Yan, H.: Microphysical effects determine macrophysical response for aerosol impacts on deep convective clouds, P. Natl. Aacad. Sci. USA, 110, E4581–E4590, https://doi.org/10.1073/pnas.1316830110, 2013.

Fan, X., Liu, J., Zhang, F., Chen, L., Collins, D., Xu, W., Jin, X., Ren, J., Wang, Y., Wu, H., Li, S., Sun, Y., and Li, Z.: Contrasting size-resolved hygroscopicity of fine particles derived by HTDMA and HR-ToF-AMS measurements between summer and winter in Beijing: the impacts of aerosol aging and local emissions, Atmos. Chem. Phys., 20, 915–929, https://doi.org/10.5194/acp-20-915-2020, 2020.

Fountoukis, C. and Nenes, A.: Continued development of a cloud droplet formation parameterization for global climate models, J. Geophys. Res., 110, D11212, https://doi.org/10.1029/2004JD005591, 2005.

Genz, C., Schrödner, R., Heinold, B., Henning, S., Baars, H., Spindler, G., and Tegen, I.: Estimation of cloud condensation nuclei number concentrations and comparison to in situ and lidar observations during the HOPE experiments, Atmos. Chem. Phys., 20, 8787–8806, https://doi.org/10.5194/acp-20-8787-2020, 2020.

Ghan, S., Chung, C., and Penner, J.: A parameterization of cloud droplet nucleation part I: single aerosol type, Atmos. Res., 30, 198–221, https://doi.org/10.1016/0169-8095(93)90024-I, 1993.

Gunthe, S. S., King, S. M., Rose, D., Chen, Q., Roldin, P., Farmer, D. K., Jimenez, J. L., Artaxo, P., Andreae, M. O., Martin, S. T., and Pöschl, U.: Cloud condensation nuclei in pristine tropical rainforest air of Amazonia: size-resolved measurements and modeling of atmospheric aerosol composition and CCN activity, Atmos. Chem. Phys.,

9, 7551–7575, https://doi.org/10.5194/acp-9-7551-2009, 2009.

Kalkavouras, P. , Bougiatioti, A. , Kalivitis, N. , Stavroulas, I. , and Mihalopoulos, N.: Regional new particle formation as modulators of cloud condensation nuclei and cloud droplet number in the eastern mediterranean. Atmos. Chem. Phys., 19(9), 6185-6203, https://doi.org/10.5194/acp-19-6185-2019,2019

Kalkavouras, P., Bossioli, E., Bezantakos, S., Bougiatioti, A., Kalivitis, N., Stavroulas, I., Kouvarakis, G., Protonotariou, A. P., Dandou, A., Biskos, G., Mihalopoulos, N., Nenes, A., and Tombrou, M.: New particle formation in the southern Aegean Sea during the Etesians: importance for CCN production and cloud droplet number, Atmos. Chem. Phys., 17, 175–192, https://doi.org/10.5194/acp-17-175-2017, 2017.

Kazil, J., Stier, P., Zhang, K., Quaas, J., Kinne, S., O'Donnell, D., Rast, S., Esch, M., Ferrachat, S., Lohmann, U., Feichter, J.: Aerosol nucleation and its role for clouds and Earth's radiative forcing in the aerosol-climate model ECHAM5-HAM, Atmos. Chem. Phys., 2010, 10, 10733, https://doi.org/10.5194/acp-10-10733-2010

Kerminen, V. M., Paramonov, M., Anttila, T., Riipinen, I., Fountoukis, C., Korhonen, H., Asmi, E., Laakso, L., Lihavainen, H., Swietlicki, E., Svenningsson, B., Asmi, A., Pandis, S. N., Kulmala, M., and Petäjä, T.: Cloud condensation nuclei production associated with atmospheric nucleation: a synthesis based on existing literature and new results, Atmos. Chem. Phys., 12, 12037-12059, https://doi.org/10.5194/acp-12-12037-2012, 2012.

Kerminen, V. M., Chen, X., Vakkari, V., Petäjä, T., Kulmala, M., and Bianchi, F.: Atmospheric new particle formation and growth: review of field observations, Environ. Res. Lett., 13, 103003, doi.org/10.1088/1748-9326/aadf3c, 2018.

Khvorostyanov, V. I., and Curry, J. A.: A simple analytical model of aerosol properties with account for hygroscopic growth: 1. Equilibrium size spectra and cloud condensation nuclei activity spectra, J. Geophys. Res., 104, 2175-2184, 1999.

Köhler, H.: The nucleus in and the growth of hygroscopic droplets[J]. Transactions of the Faraday Society, 1936, 32:

1152-1161.

Kulmala, M., Kerminen, V. M.: On the formation and growth of atmospheric nanoparticles[J]. Atmospheric Research, 2008, 90(2-4):132-150.

Kulmala, M., Petäjä, T., Nieminen, T., Sipilä, M., Manninen, H. E., Lehtipalo, K., Dal, Maso, M., Aalto, P., Junninen, H., Paasonen, P., Riipinen, I., Lehtinen, K. E. J., Laaksonen, A., and Kerminen, V.-M.: Measurement of the nucleation of atmospheric aerosol particles, Nat. Protocol., 7, 1651–1667, https://doi.org/10.1038/nprot.2012.091, 2012.

Leaitch, W. R., Strapp, J. W., and Isaac, G. A.: Cloud droplet nucleation and cloud scavenging of aerosol sulphate in polluted atmospheres, Tellus, 38B, 328–344, 1986

Leino, K., Nieminen, T., Manninen, H. E., Petäjä, T., Kerminen, V. M., and Kulmala, M.: Intermediate ions as a strong indicator of new particleformation bursts in a boreal forest, Boreal Environ. Res., 21, 274-286, 2016.

Li Y., Zhang F*., Li Z., Sun L., Wang Z., Li P., Sun Y., Ren J., Wang Y. and Cribb M.: Influences of aerosol physiochemical properties and new particle formation on CCN activity from observation at a suburban site of China, Atmos. Res., 188, 80-89, 2017.

Li, Z., Niu, F., Fan, J. et al. Long-term impacts of aerosols on the vertical development of clouds and precipitation. Nature Geosci 4, 888–894 (2011). https://doi.org/10.1038/ngeo1313

Liu, C., Wang, T., Rosenfeld, D., Zhu, Y., Yue, Z., Yu, X.: Anthropogenic effects on cloud condensation nuclei distribution and rain initiation in East Asia. Geophysical Research Letters, 47, e2019GL086184.https://doi.org/10.1029/2019GL086184,2019.

Ma, N., Zhao, C., Tao, J., Wu, Z., Kecorius, S., Wang, Z., Größ, J., Liu, H., Bian, Y., Kuang, Y., Teich, M., Spindler, G., Müller, K., van Pinxteren, D., Herrmann, H., Hu, M., and Wiedensohler, A.: Variation of CCN activity during new particle formation events in the North China Plain, Atmos. Chem. Phys., 16, 8593–8607,

https://doi.org/10.5194/acp-16-8593-2016, 2016.

Merikanto, J., Spracklen, D. V., Pringle, K. J., and Carslaw, K. S.: Effects of boundary layer particle formation on cloud droplet number and changes in cloud albedo from 1850 to 2000, Atmos. Chem. Phys., 10, 695–705, https://doi.org/10.5194/acp-10-695-2010, 2010.

Morales, R. and Nenes, A.: Characteristic updrafts for computing distribution-averaged cloud droplet number and stratocumulus cloud properties, J. Geophys. Res., 115, D18220, https://doi.org/10.1029/2009JD013233, 2010.

Morales-Betancourt, R., Nenes, A.: Understanding the contributions of aerosol properties and parameterization discrepancies to droplet number variability in a global climate model. Atmos Chem Phys 14(9):4809–4826,2014.

Nenes, A. and Seinfeld, J. H.: Parameterization of cloud dropletformation in global climate models, J. Geophys. Res, 108, 4415, https://doi.org/10.1029/2002JD002911, 2003.

Nenes, A., Chan, S., Abdul-Razzak, H., Chuang, P., and Seinfeld, J. H.: Kinetic limitations on cloud droplet formation and impact on cloud albedo, Tellus 53B, 133–149, https://doi.org/10.3402/tellusb.v53i2.16569, 2001.

Ng, N. L., Herndon, S. C., Trimborn, A., Canagaratna, M. R., Croteau, P. L., Onasch, T. B.: An aerosol chemical speciation monitor (ACSM) for routine monitoring of the composition and mass concentrations of ambient aerosol, Aerosol Science and Tech, 2011, 45(7):780-794, https://doi.org/10.1080/02786826.2011.560211, 2011.

Paasonen, P., Peltola, M., Kontkanen, J., Junninen, H., Kerminen, V.-M., and Kulmala, M.: Comprehensive analysis of particle growth rates from nucleation mode to cloud condensation nuclei in boreal forest, Atmos. Chem. Phys., 18, 12085–12103, https://doi.org/10.5194/acp-18-12085-2018, 2018.

Peng, J. F., Hu, M., Wang, Z. B., Huang, X. F., Kumar, P., Wu, Z. J., Guo, S., Yue, D. L., Shang, D. J., Zheng, Z., and He, L. Y.: Submicron aerosols at thirteen diversified sites in China: size distribution, new particle formation and corresponding contribution to cloud condensation nuclei production, Atmos. Chem. Phys., 14, 10249–10265, https://doi.org/10.5194/acp-14-10249-2014, 2014.

Peng,Y., Dong, Y., Li, X. M.: Different Characteristics of New Particle Formation Events at Two Suburban Sites in Northern China[J]. Atmosphere, 2017, 8(12):258, https://doi.org/10.3390/atmos8120258.

Petters, M. D. and Kreidenweis, S. M.: A single parameter representation of hygroscopic growth and cloud condensation nucleus activity, Atmos. Chem. Phys., 7, 1961–1971, https://doi.org/10.5194/acp-7-1961-2007, 2007.

Ramanathan, V., Crutzen, P. J., Kiehl, J. T., and Rosenfeld, D.: Aerosols, climate, and the hydrological cycle, Science, 294, 2119–2124, https://doi.org/10.1126/science.1064034, 2001.

Ren, J., Zhang, F., Wang, Y., Collins, D., Fan, X., Jin, X., Xu, W., Sun, Y., Cribb, M., and Li, Z.: Using different assumptions of aerosol mixing state and chemical composition to predict CCN concentrations based on field measurements in urban Beijing, Atmos. Chem. Phys., 18, 6907–6921, https://doi.org/10.5194/acp-18-6907-2018, 2018.

Rose, C., Sellegri, K., Moreno, I., Velarde, F., Ramonet, M., Weinhold, K., Krejci, R., Andrade, M., Wiedensohler, A., Ginot, P., and Laj, P.: CCN production by new particle formation in the free troposphere, Atmos. Chem. Phys., 17, 1529–1541, https://doi.org/10.5194/acp-17-1529-2017, 2017.

Seinfeld, J. H., Bretherton, C. S., Carslaw, K. S., Coe, H., DeMott, P. J., Dunlea, E. J., Feingold, G., Ghan, S. J., Guenther, A.B., Kahn, R. A., Kracunas, I. P., Kreidenweis, S. M., Molina, M. J., Nenes, A., Penner, J. E., Prather, K. A., Ramanathan, V., Ramaswamy, V., Rasch, P. J., Ravishankara, A. R., Rosenfeld, D., Stephens, G., and Wood R.: Improving Our Fundamental Understanding of the Role of Aerosol-Cloud Interactions in the Climate System, P. Nat. Acad. Sci. USA, 113, 5781–5790, https://doi.org/10.1073/pnas.1514043113, 2016.

Spracklen, D. V., Carslaw, K. S., Merikanto, J., Mann, G. W., Reddington, C. L., Pickering, S., Ogren, J. A., Andrews, E., Baltensperger, U., Weingartner, E., Boy, M., Kulmala, M., Laakso, L., Lihavainen, H., Kivekäs, N., Komppula, M., Mihalopoulos, N., Kouvarakis, G., Jennings, S. G., O'Dowd, C., Birmili, W., Wiedensohler, A., Weller, R., Gras, J., Laj, P., Sellegri, K., Bonn, B., Krejci, R., Laaksonen, A., Hamed, A., Minikin, A., Harrison, R. M., Talbot,

R., and Sun, J.: Explaining global surface aerosol number concentrations in terms of primary emissions and particle formation, Atmos. Chem. Phys., 10, 4775–4793, https://doi.org/10.5194/acp-10-4775-2010, 2010.

Sullivan, S. C., Lee, D., Oreopoulos, L., and Nenes, A.: The role of updraft velocity in temporal variability of cloud hydrometeor number, P. Natl. Acad. Sci. USA, 113, 5781–5790, https://doi.org/10.1073/pnas.1514043113, 2016.

Sun, Y. L., Wang, Z. F., Du, W., Zhang, Q., Wang, Q. Q., Fu, P. Q., Pan, X. L., Li, J., Jayne, J., and Worsnop, D. R.: Longterm real-time measurements of aerosol particle composition in Beijing, China: seasonal variations, meteorological effects, and source analysis, Atmos. Chem. Phys., 15, 10149–10165, https://doi.org/10.5194/acp-15-10149-2015, 2015.

Twomey, S.: The influence of pollution on the shortwave albedo of clouds, J. Atmos. Sci., 34, 1149–1152, 1977.

Wang, S. C. and Flagan, R. C.: Scanning Electrical Mobility Spectrometer, Aerosol Sci. Tech., 13, 230–240, 1990.

Wang Y., Zhang F., Li Z., Tan H., Xu H., Ren J., Zhao J., Du W. and Sun Y.: Enhanced hydrophobicity and volatility of submicron aerosols under severe emission control conditions in Beijing, Atmos Chem Phys, 17, 5239-5251, 10.5194/acp-17-5239-2017, 2017.

Wiedensohler, A., Birmili, W., Nowak, A., Sonntag, A., Weinhold, K., Merkel, M., Wehner, B., Tuch, T., Pfeifer, S.: Mobility particle size spectrometers: harmonization of technical standards and data structure to facilitate high quality long-term observations of atmospheric particle number size distributions, Atmos. Meas. Tech., 5, 657–685, https://doi.org/10.5194/amt-5-657-2012, 2012.

Wiedensohler, A., Chen, Y. F., Nowak, A., Wehner, B., Achtert, P., Berghof, M., Birmili, W., Wu, Z. J., Hu, M., Zhu, T., Takegawa, N., Kita, K., Kondo, Y., Lou, S. R., Hofzumahaus, A., Holland, F., Wahner, A., Gunthe, S. S., Rose, D., Su, H., and Pöschl, U.: Rapid aerosol particle growth and increase of cloud condensation nucleus activity by secondary aerosol formation and condensation: A case study for regional air pollution in northeastern China, J. Geophys. Res., 114, D00G08, https://doi.org/10.1029/2008JD010884, 2009.

Wu, Z., Hu, M., Liu, S., Wehner, B., and Wiedensohler, A.: Particle number size distribution in the urban atmosphere of Beijing, China, Atmos. Environ., 42, 7967–7980, 2008.

Wu, Z. J., Hu, M., Yue, D. L.: Evolution of particle number size distribution in an urban atmosphere during episodes of heavy pollution and new particle formation. Sci China Earth Sci, 2011, 54, doi: 10.1007/s11430-011-4227-9,2011.

Wu, Z. J., Poulain, L., Birmili, W., Größ, J., Niedermeier, N., Wang, Z. B., Herrmann, H., and Wiedensohler, A.: Some insights into the condensing vapors driving new particle growth to CCN sizes on the basis of hygroscopicity measurements, Atmos. Chem. Phys., 15, 13071–13083, https://doi.org/10.5194/acp-15-13071-2015, 2015.

Yue, D. L., Hu, M., Zhang, R. Y., Wu, Z. J., Su, H., Wang, Z. B., Peng, J. F., He, L. Y., Huang, X. F., Gong, Y. G., Wiedensohler, A.: Potential contribution of new particle formation to cloud condensation nuclei in Beijing[J]. Atmospheric Environment, 2011, 45(33):6070-6077, https://doi.org/10.1016/j.atmosenv.2011.07.037.

Zimmerman, A. , Petters, M. D. , & Meskhidze, N.: Observations of new particle formation, modal growth rates, and direct emissions of sub-10 nm particles in an urban environment. Atmospheric Environment, 242, 117835.

Zhang, F., Li, Y., Li, Z., Sun, L., Li, R., Zhao, C., Wang, P., Sun, Y., Liu, X., Li, J., Li, P., Ren, G., and Fan, T.: Aerosol hygroscopicity and cloud condensation nuclei activity during the AC3Exp campaign: implications for cloud condensation nuclei parameterization, Atmos. Chem. Phys., 14, 13423–13437, https://doi.org/10.5194/acp-14-13423-2014, 2014.

Zhang, F., Li, Z., Li, Y., Sun, Y., Wang, Z., Li, P., Sun, L., Wang, P., Cribb, M., Zhao, C., Fan, T., Yang, X., and Wang, Q.: Impacts of organic aerosols and its oxidation level on CCN activity from measurement at a suburban site in China, Atmos. Chem. Phys., 16, 5413–5425, https://doi.org/10.5194/acp-16-5413-2016, 2016.

Zhang, F., Wang, Y., Peng, J., Ren, J., Collins, D., Zhang, R., … Li, Z.: Uncertainty in predicting CCN activity of aged and primary aerosols. Journal of Geophysical Research: Atmospheres, 122, 11,723–11,736.

https://doi.org/10.5194/acp-2021-23
Preprint. Discussion started: 1 March 2021

https://doi.org/10.1002/2017JD027058.

Zhang, F., Ren, J., Fan, T., Chen, L., Xu, W., Sun, Y.: Significantly enhanced aerosol CCN activity and number concentrations by nucleation-initiated haze events: A case study in urban Beijing. J. Geophys. Res.-Atmos., 124. https://doi.org/10.1029/ 2019JD031457, 2019

Zheng, Y. T.,Rosenfeld, D.,Li, Z. Q.: Satellite Inference of Thermals and Cloud-Base Updraft Speeds Based on Retrieved Surface and Cloud-Base Temperatures[J], Journal of the Atmospheric Sciences,2015,72(6), https://doi.org/10.1175/JAS-D-14-0283.1,201